CANCER GENOMICS & PROTEOMICS *13*: 443-452 (2016)
doi:10.21873/cgp.20007

Characterization of Heparan Sulfate Proteoglycan-positive Recycling Endosomes Isolated from Glioma Cells

KATARZYNA A. PODYMA-INOUE, TAKUYA MORIWAKI, ANUPAMA R. RAJAPAKSHE, KAZUE TERASAWA and MIKI HARA-YOKOYAMA

Department of Biochemistry, Graduate School of Medical and Dental Sciences, Tokyo Medical and Dental University (TMDU), Tokyo, Japan

Abstract. *Background: Heparan sulfate proteoglycans (HSPGs)-dependent endocytic events have been involved in glioma progression. Thus, comprehensive understanding of the intracellular trafficking complexes formed in presence of HSPGs would be important for development of glioma treatments. Materials and Methods: Subcellular fractionation was used to separate vesicles containing HSPGs from the rat C6 glioma cell line. Isolated HSPG-positive vesicles were further characterized with liquid chromatography-mass spectrometry. Results: The HSPG-positive vesicular fractions, distinct from plasma membrane-derived material, were enriched in endocytic marker, Rab11. Proteomic analysis identified more than two hundred proteins to be associated with vesicular membrane, among them, over eighty were related to endosomal uptake, recycling or vesicular transport. Conclusion: Part of HSPGs in glioma cells is internalized through clathrin-dependent endocytosis and undergo recycling. The development of compounds regulating HSPG-mediated trafficking will likely enable design of effective glioma treatment.*

Malignant gliomas are common and devastating brain tumors that frequently have poor prognosis (1). Heparan sulfate proteoglycans (HSPGs) are important players in glioma invasion and thus have potential as therapeutic target. HSPGs are widely expressed by animal cells being one of the important constituents of extracellular matrix and plasma membranes. HSPGs comprise of protein core with covalently attached heparan sulfate chains consisting of repeating disaccharide units containing N-acetyl-glucosamine and glucuronic acid. They intercept and regulate biological signals coming into cells, serving as receptors for a variety of extracellular ligands; including growth factors, cytokines, chemokines, or enzymes (2, 3). Cell surface HSPGs (represented by syndecan and glypican families) participate in endocytic processes, playing a significant role in both constitutive- and receptor-mediated endocytosis (4). HSPG-dependent uptake of various extracellular ligands and morphogens has been reported to provide the mechanism for removal of bioactive molecules from the extracellular environment, forming their concentration gradient or delivering them to the cytoplasm (5), suggesting an importance of HSPG in glioma progression.

The ability of HSPGs to regulate the accessibility of oncogenic ligands, activity and localization of their receptors likely contributes to glioma progression. Indeed, many studies have pointed the role of HSPGs as co-receptors in presentation of growth factors to their receptors and involvement of HSPG-related signals in glioma pathogenesis. For example, overexpression of glypican-1 detected in human glioma cell line was found to be increased in FGF-2-related signals resulting in growth stimulation (6). Other studies by Xu and colleagues revealed that up-regulated synthesis of syndecan-1 was found in patients with poor prognosis and seemed to be correlated with tumor progression (7). It has been suggested that HSPGs promote tumor growth by facilitating formation of ligand-receptor tyrosine kinase signaling complexes as well as their endocytic clearance and fate (8). Thus, aiming at developing compounds that regulate HSPG-mediated trafficking will likely enable design of glioma treatment. Although the importance of HSPG-mediated endocytosis is well recognized and has been well studied in terms of their catabolic pathways (9, 10), there have been only few studies focusing on the characterization of HSPG-dependent trafficking using HeLa or kidney cell (11). Based on that report, it seems that HSPG-mediated endocytosis is not restricted to only one pathway, but rather involves various

Correspondence to: Katarzyna A. Podyma-Inoue, Department of Biochemistry, Graduate School of Medical and Dental Sciences, Tokyo Medical and Dental University (TMDU), 1-5-45 Yushima, Bunkyo-ku, Tokyo 113-8549, Japan. Tel: +81 358035449; Fax: +81 358030187, e-mail: kapobch@tmd.ac.jp

Key Words: Proteomics, heparan sulfate proteoglycan, Rab11, transport vesicle.

routes; (*i.e.*, clathrin- and caveolin-dependent pathways), that are likely to depend on the nature of internalized ligands (11). Involvement of lipid rafts has been suggested, but the exact mechanisms underlying endocytic event and characterization of key player molecules remain unclear (12). There were no attempts leading to identification of molecules participating in HSPG-dependent endocytic complexes or involved in HSPG-dependent trafficking in glioma cells.

Considering the importance of HSPG in glioma progression and its role as a receptor for endocytosis, we attempted the characterization of the intracellular trafficking complexes formed in the presence of HSPGs in a rat C6 glioma cell line model. Using subcellular fractionation, we isolated HSPG-positive transport vesicles and found them to be enriched in Rab11, a small GTPase that is involved in vesicular transport. The detailed proteomic analysis of HSPG-positive and Rab11-rich vesicles identified over eighty proteins related to vesicular transport; *i.e.* endocytosis or recycling. Interestingly, our study also revealed the association of these HSPG-positive transport vesicles with vimentin, suggesting that intracellular trafficking in C6 glioma cells may partially depend on intermediate filaments. Targeting HSPG-mediated trafficking by development of compounds interfering with formation of HSPG-dependent endocytic complexes or regulating HSPG-mediated endocytic pathways will likely enable efficient glioma treatment.

Materials and Methods

Antibodies and reagents. Heparitinase (*Flavobacterium heparinum*, #100703) and chondroitinase ABC (*Proteus vulgaris*, #100332), a mouse monoclonal anti-heparan sulfate antibody (F69-3G10, #3700260) recognizing HS neo-epitope generated by digestion of HS with heparitinase and a mouse monoclonal anti-heparan sulfate antibody (F58-10E4, #370255) were all purchased from Seikagaku Corporation (Tokyo Japan). A guinea pig anti-vimentin antibody (GP53) was from Progen (Heidelberg, Germany). For detection of various organelle markers the following antibodies were used: a mouse monoclonal anti-α1 sodium-potassium ATPase, Na^+-K^+-ATPase antibody (ab7671, Abcam, Cambridge, UK), a rabbit polyclonal anti-Rab11 antibody (ab3612, Abcam, Cambridge, UK), a mouse polyclonal anti-Rab5 (#610282, BD Transduction Laboratories, San Jose, CA, USA), a mouse monoclonal anti-Golgi SNARE 28 (G83820, BD Transduction Laboratories, San Jose, CA, USA) and a rabbit polyclonal anti-protein disulfide isomerase family A, member 3, PDIA3 antibodies (HPA003230, Sigma, St. Louis, MO, USA). Other materials were of the highest grade commercially available.

Cell culture. The rat C6 glioma cell line (RCB2854), obtained from the RIKEN Bioresource Center (Tsukuba, Ibaraki, Japan) was cultured in RPMI1640 medium (R8758, Sigma-Aldrich, St. Louis, MO, USA), supplemented with 10% fetal bovine serum in the presence of penicillin (50 U/mL), and streptomycin (50 μg/mL), at 37˚C under 95% air/5% CO_2 atmosphere.

Purification of proteoglycans from cultured cells. Confluent C6 cells cultured in T-175 flasks were washed twice with ice-cold phosphate-buffered saline (PBS) and subjected to proteoglycan purification as described previously (13). Briefly, cells were extracted overnight in 4 M guanidine HCl, 2% Triton X-100, at 4˚C. Extraction buffer was exchanged on Sephadex-G50 column equilibrated with 8 M urea, 0.2 M NaCl, 0.2 M sodium acetate, pH 6.8, containing 0.5% Triton X-100. Proteoglycans recovered from the excluded volume of Sephadex G-50, were bound to Q-Sepharose slurry and packed into a column. After extensive wash, the bound material was eluted with 4 M guanidine HCl, 0.5%Triton X-100, dialyzed against PBS, treated with heparitinase and used in immunoblotting analysis. The same protocol was applied to rat parathyroid cells used as positive control in subsequent immunoblotting analysis.

Immunocytochemistry. C6 cells were cultured in 12-well plates on 15-mm diameter round glass coverslips. Before fixation, cells were incubated with Hoechst 33342 (final concentration 1 μg/ml) for 30 min, fixed with 4% PFA for 10 min at room temperature, washed with PBS containing 0.1 M glycine, and permeabilized with 0.1% Triton X-100 in PBS for 5 min at room temperature. Subsequently, cells were blocked with 1% BSA in PBS for 30 min and stained with primary antibodies recognizing HSPG (10E4; 1:200) for 1 h. To visualize stained molecules, cells were incubated with the secondary antibodies, Alexa Fluor 555-conjugated anti-mouse IgM antibody (1:400), for 1 h at room temperature. After an excessive wash, coverslips were mounted using Prolong Gold Mounting Reagent (Invitrogen Life Technologies, Eugene, OR, USA) and observed under a fluorescent microscope FV10i (Olympus, Tokyo, Japan).

RT-PCR analysis. Rat C6 glioma cells were grown in 35-mm diameter dish until confluence under the conditions described above. Total RNA was isolated with RNA STAT-60 reagent (TELL-TEST, Friendswood, TX, USA) based on the protocol suggested by the manufacturer, followed by reverse transcriptase reaction using Superscript III Reverse Transcriptase (Life Technologies, Carlsbad, CA, USA) under the conditions suggested by the manufacturer. Expression of syndecans 1-4 mRNAs was determined with the specific set of primers reported previously (13). Primers used for analysis of glypicans 1-6 mRNA expression and nucleotide sequence data used for primer design are listed in Table I. Amplification reaction was carried out under the following conditions: initial denaturation step at 94˚C for 3 min followed by 30 cycles of denaturation step at 94˚C, 30 sec; annealing step at 64˚C for 45 sec and extension step at 72˚C for 60 sec, with a final extension step at 72˚C for 2 min. All amplified products were then electrophoresed on 2% agarose gel in TAE buffer, visualized by ethidium bromide and photographed under UV transillumination.

Subcellular fractionation using OptiPrep® gradient ultracentrifugation. Rat C6 glioma cells (1×10^7) in five 100-mm diameter dishes were grown until confluence, washed extensively with ice-cold PBS, scraped and collected by centrifugation. Cells were re-suspended in ice-cold 10 mM Tris-HCl pH 7.4 homogenization buffer containing 1 mM EDTA, 0.25 mM sucrose, 1 mM EGTA and Halt Protease Inhibitor Cocktail (PIERCE, Rockford, IL, USA) at a ratio of 4 ml of homogenization buffer per 1 g of collected cells. Cell suspension was disrupted with Potter homogenizer, followed by several strokes through 25-gauge needle and subjected to

Table I. *List of primers specific for rat glypican family used in RT-PCR analysis.*

Gene-specific primers	Primer sequence	GeneBank accession no.
Glypican-1		NM_030828
Glp1-forward	5'-CAGTGACGTAGTCCGAAAGGTG-3'	
Glp1-reverse	5'-GTGTGTCCTTGTTGTCCTGGAG-3'	
Glypican-2		NM_138511
Glp2-forward	5'-CCTTACTCGGCTCACTTCAACT-3'	
Glp2-reverse	5'-GATCTTCACCCCTATGGACTCA-3'	
Glypican-3		NM_012774
Glp3-forward	5'-ATGAATTGTTCGACAGCCTCTT-3'	
Glp3-reverse	5'-CACATACTGGATGGAATCATGG-3'	
Glypican-4		NM_001014108
Glp4-forward	5'-CTCAAACATCATGAGAGGCTGT-3'	
Glp4-reverse	5'-CAGTAACCAGTCGGTCCAAACT-3'	
Glypican-5		XM_224489
Glp5-forward	5'-CATGGCTCCAAGTTGTCAGTTA-3'	
Glp5-reverse	5'-GCTGAACAGTGGTTTCCTCTCT-3'	
Glypican-6		XM_577463
Glp6-forward	5'-TGCGAAGTAACATTCTGCTTGT-3'	
Glp6-reverse	5'-TGTTGGCTTAACTTGTCTTCCA-3'	

centrifugation at 1,000 × *g* for 10 min, at 4˚C to remove nuclear fraction. Post-nuclear supernatant was then subjected to fractionation using OptiPrep gradient ultracentrifugation. OptiPrep (iodixanol) solutions of 2.5, 5.0, 7.5, 10.0, 12.5, 15.0, 17.5 and 20% were prepared by diluting 50% working OptiPrep solution with homogenization buffer. Obtained solutions (800 µl each) were layered to form discontinuous iodixanol gradient. Post-nuclear supernatant was then applied on the top of the gradient and centrifuged at 40,000 rpm, 4˚C for 2 h (RPS65T rotor, Hitachi Koki, Tokyo, Japan). Sixteen fractions of equal volume were collected from the top of the gradient for further analysis. Each fraction was assayed for protein content (BCA Protein Assay Kit, Pierce, Friendswood, IL, USA) and iodixanol density followed by immunoblotting to determine distribution of various organelle markers.

For detection of proteoglycans, samples were collected by ultracentrifugation at 50,000 rpm and 4˚C for 30 min in TLA 100.2 rotor (Beckmann, Fullerton, CA, USA) and treated with heparitinase prior to western blotting analysis. The enzymatic reaction was carried out at 37˚C for 2 h, in 0.1 M Tris-acetate, 10 mM calcium acetate buffer, pH 7.3, in the presence of 1 µU of the enzyme.

Immunoblot analysis. Purified proteoglycans or samples obtained from subcellular fractionations were separated on 5-20% gradient polyacrylamide gels (Wako, Osaka, Japan) under reducing conditions according to the method of Laemmli (14). Following electrophoresis, proteins were transferred overnight onto a PVDF membrane and subjected to immunoblotting. Briefly, membranes were blocked with 1% BSA in PBS for 40 min and incubated with specific primary antibodies for 3 h at room temperature. After six washes with PBS, 0.1% Tween-20, membranes were incubated with appropriate HRP-conjugated secondary antibodies and washed several times with PBS, 0.1% Tween-20. Binding of specific antibodies was detected using ECL or ECL Prime reaction (RPN2109, GE Healthcare, Buckinghamshire, UK).

Mass spectrometry analysis. Fractions rich in vesicles positive for both HSPG and Rab11 were depleted from cytoplasmic proteins by ultracentrifugation at 50,000 rpm and 4˚C for 30 min in TLA 100.2 rotor (Beckmann, Fullerton, CA, USA), separated on 5-20% gradient polyacrylamide gels and stained with Protein Silver Staining Kit II (Wako, Osaka, Japan). Cut-out gel pieces were then destained with 25 mM ammonium bicarbonate in 30% acetonitrile, followed by dehydration in acetonitrile using centrifugal evaporator. After subsequent reduction with 20 mM dithiothreitol in100 mM ammonium bicarbonate for 1 h, proteins within the gels were alkylated using 54 mM iodoacetamide in 100 mM ammonium bicarbonate for 1 h, and washed with 5% acetic acid in 50% methanol followed by 100 mM ammonium bicarbonate and final dehydration with acetonitrile. Such prepared gels were then subjected to overnight in-gel-digestion with trypsin (B5111, sequencing grade, Promega, Madison, WI, USA) at 37˚C. Obtained peptides were then analyzed using LC-MS analysis system (Brüker, Billerica, MA, USA) equipped with nano-UHPLC system (combination of Magic C18AQ capillary column preceded by NanoTrap column) connected to Maxis-4G-CPR mass spectrometer with nano-ESI source. Searches of database were done using ProteinScape 3.1 Software on Mascot 2.5.1 (Matrix Science).

Results

Multiple types of HSPGs were detected in C6 glioma cells. In order to study HSPG-dependent trafficking in glioma, we used the rat C6 glioma cell line, a well-characterized glioma cell model. First, rat C6 glioma cells were analyzed for expression of HSPG using antibodies reactive to heparan sulfate (HS). Immunocytochemical analysis revealed strong staining confirming the presence of HSPG (Figure 1A). To determine the type of HSPGs expressed by C6 glioma cells, the expression of all reported members of syndecan and

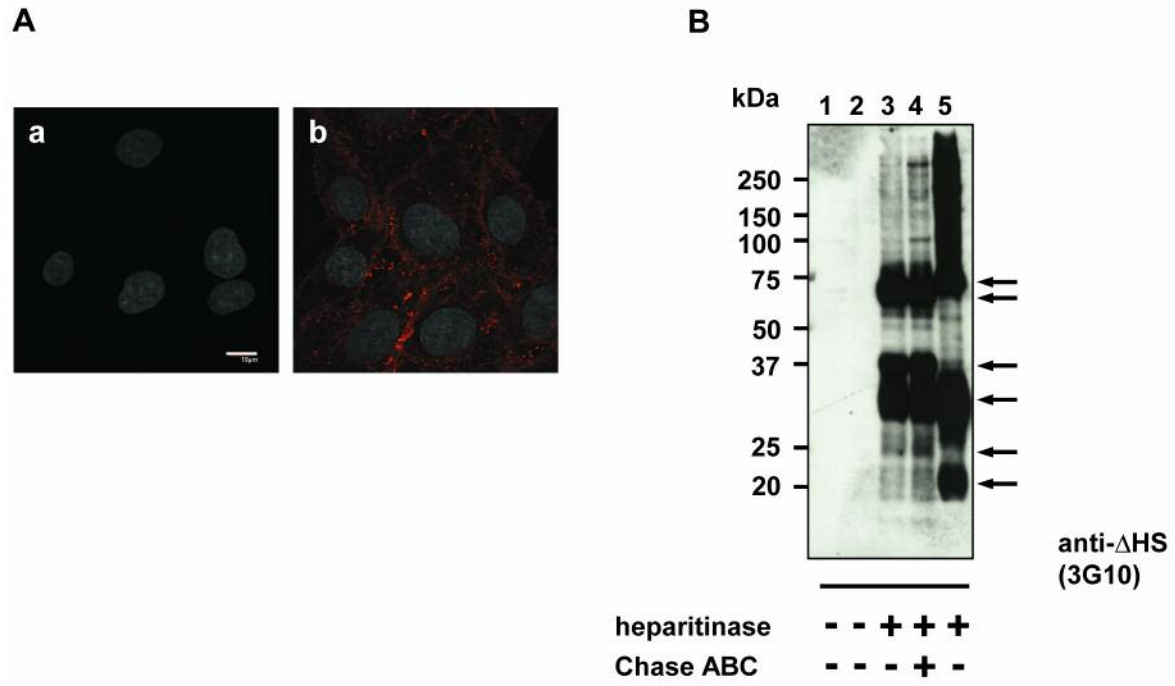

Figure 1. *High levels of HSPGs expression can be detected in C6 glioma cells. The C6 glioma cell line was analyzed for expression of HSPGs. (A) Immunocytochemistry was performed using heparan sulfate-specific antibodies. C6 cells were cultured, fixed with PFA, and stained with 10E4 antibody (b) or with secondary antibodies only (a). The nuclei were stained with Hoechst 33342. Scale bars: 10 μm. (B) Proteoglycans isolated from confluent C6 glioma cells were purified on Q-Sepharose, incubated with or without heparitinase and immunoblotted with anti-ΔHS antibodies (3G10). Lanes: 1, digestion buffer only; 2, 3, 4 correspond to purified material from C6 glioma cells; 5, positive control for immunoblotting representing rat parathyroid proteoglycans.*

glypican families were analyzed. RT-PCR revealed the expression of all known syndecans, syndecan-1, syndecan-2, syndecan-3 and syndecan-4, and three glypicans; glypican-1, glypican-3 and glypican-4 (Figure 2). The presence of multiple HSPGs in C6 cells was also confirmed with immunoblotting. Analysis of partially purified proteoglycans with the 3G10 antibodies, recognizing epitopes generated after cleavage of HS chains with heparitinase, revealed expression of several core proteins being modified with HS chains with apparent molecular weights of 75, 65, 37, 30, 25 and 20 kDa respectively (Figure 1B). The detected pattern was not changed by additional treatment with chondroitinase ABC (Figure 1B, lane 4) suggesting HS chains to be a main GAG modification of detected protein cores.

Low-density vesicular fractions positive for HSPGs were characterized by the presence of Rab11 and Rab5. HSPGs play an important role in the internalization of many extracellular ligands. Both clathrin-dependent and clathrin-independent pathways are involved, but key player molecules and the fate of internalized complexes remain unclear. In the next step, we attempted to characterize transport vesicles present in C6 glioma cells. The post-nuclear supernatant form C6 glioma cells was subjected to subcellular fractionation on OptiPrep gradient and analyzed with antibodies recognizing various organelle markers and antibodies reactive to HS-derived epitope, respectively. HSPG exhibited a broad distribution and could be detected in fractions 3 through 13, with the strongest signal found in fractions 9 and 10 (Figure 3). Those fractions likely corresponded to plasma membrane and Golgi-derived materials as revealed by staining pattern of plasma membrane and a Golgi marker, Na^+-K^+-ATPase and GS28, respectively (Figure 3). Low-density fraction, positive for HSPGs was found to be enriched with the small GTPases, Rab5 and Rab11, well-known regulators of intracellular vesicle transport (15), raising the possibility that this low-density material may represent transport vesicles. Thus in the next step we decided to identify proteins associated with this low-density vesicular fraction.

Proteomic analysis revealed that various transport-related proteins were associated with HSPG- and Rab11-positive compartments. HSPG and the Rab11-positive material corresponding to fractions 2 and 3 (Figure 3) was combined, depleted of cytosolic proteins and resolved by SDS-PAGE.

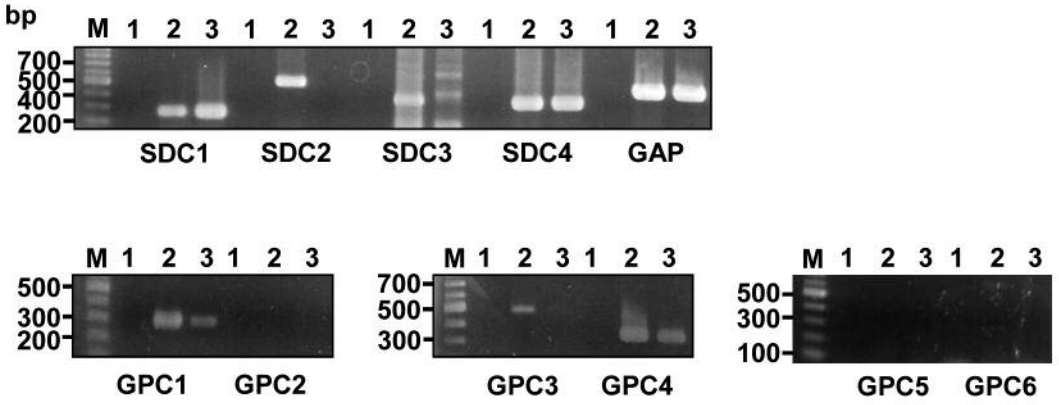

Figure 2. *RT-PCR analysis of C6 glioma cells with syndecan- and glypican-specific primers. Total RNA and cDNA was prepared from C6 glioma cells and subjected to RT-PCR analysis (refer to Materials and Methods and Table I for details). Lanes: M, 100 bp marker; 1, negative controls containing no cDNA; 2, C6 glioma cell line; 3; rat parathyroid cell line (positive control). SDC1-4: syndecan 1-4; GPC1-6: glypican 1-6.*

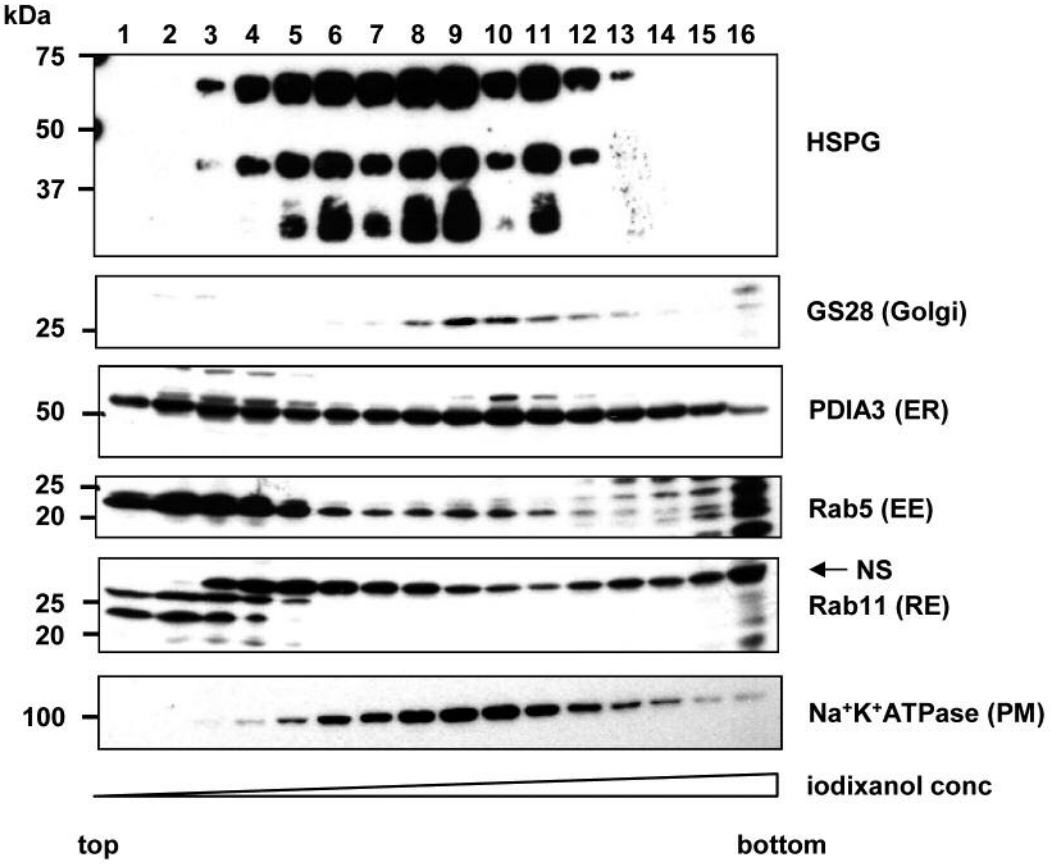

Figure 3. *Subcellular fractionation of C6 glioma cells using OptiPrep ultracentrifugation gradient. C6 glioma cells were subjected to subcellular fractionation as described in the Materials and Methods section. Each fraction was analyzed by immunoblotting with specific antibodies for organelle markers and heparan sulfate, respectively. For organelle marker detection, equal volume of each fraction (14 µl/lane) was applied on gel. Depending on the analyzed marker, the samples were run under non-reducing (Na^+-K^+-ATPase, PIDA3 and Rab11) or reducing (GS28, Rab5 and HSPGs) conditions. To detect HSPGs, 90 µl of each sample was concentrated and treated with heparitinase prior the electrophoresis. Lanes: 1-16 correspond to subcellular fractions collected from the top of the gradient. In Rab11-stained membrane, bands marked with (NS) correspond to non-specific staining also described by manufacturer in antibody data sheet.*

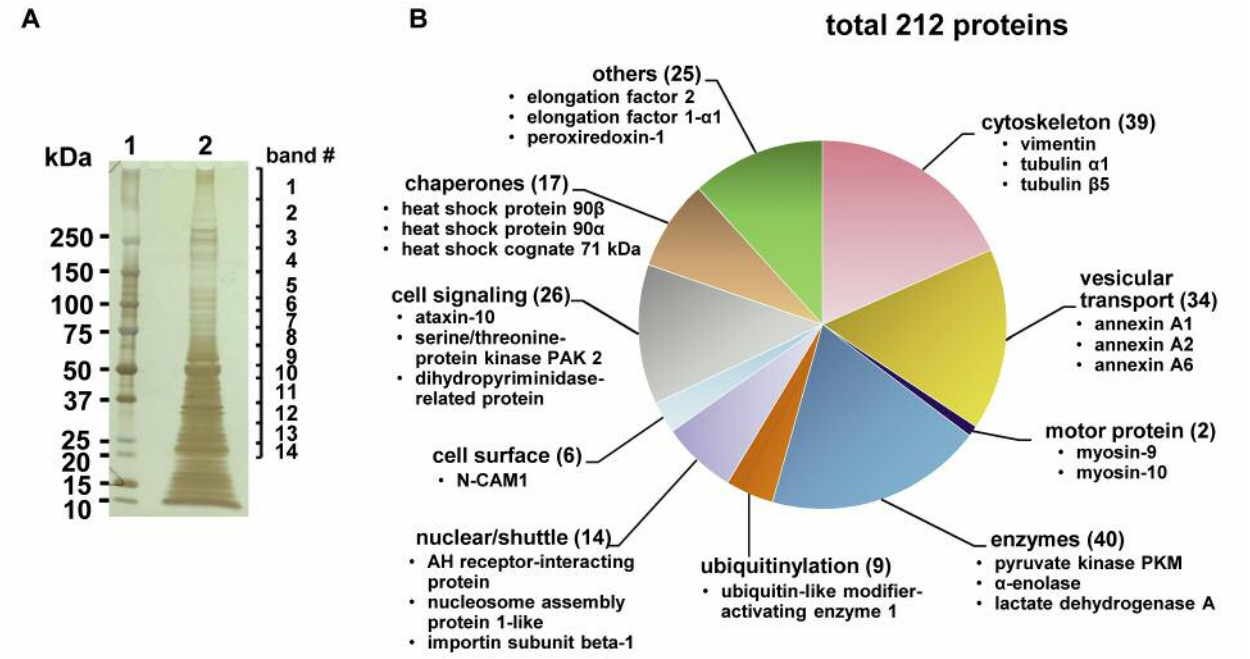

Figure 4. *Mass spectrometry analysis of proteins present in low-density vesicular fractions obtained from OptiPrep® ultracentrifugation. Fractions 2 and 3 obtained from subcellular fractionation were combined, subjected to ultracentrifugation for isolation of membrane-associated proteins and separated by SDS-PAGE. In-gel-digestion products were analyzed with LC-MS. (A) Silver staining of membrane-associated proteins resolved by SDS-PAGE. Lane 1, Molecular weight protein standard; lane 2, membrane-associated proteins from combined fractions 2 and 3. Numbers 1 through 14 correspond to gel fragments subjected to in-gel digestion. (B) Proteins identified by LC-MS analysis. A total of 212 proteins were identified and categorized into 10 groups. Numbers in brackets correspond to number of identified proteins belonging to each category. Proteins corresponding to each category, identified with the highest score and shown in the Table II are listed.*

The staining pattern showed multiple proteins to be associated with this low-density fraction (Figure 4A), among which 212 could be identified in subsequent LC-MS analysis (Figure 4B). More than eighty proteins, corresponding to 30% of total identified proteins were related to vesicular transport, representing the molecules associated with early endosomes, involved in recycling or sorting, and cytoskeletal components important for vesicular trafficking (Figure 4B) (Table II). Proteins related to vesicular transport included annexins, and Eps15 homology domain (EHD)-containing proteins which were previously implicated in regulations of endosomal trafficking (16-18). In addition, various types of Rab proteins, small GTPases known to be involved in controlling membrane transport, could be also detected. Rab-11a was also identified by proteomic analysis with high protein score (score 60.70), but it was represented only by two peptides and thus was not included in the Table II. Cytoskeleton-related proteins were represented by various types of tubulins and actin (Table II) that was in agreement with the present state of knowledge regarding the vesicular transport to be microtubules- and actin filaments-dependent (19). One of the most abundant proteins identified by our LC-MS analysis was vimentin, the member of type III intermediate filament (IF) protein family, which raised the possibility that IFs maybe involved in vesicular transport in C6 glioma. List of all proteins identified with protein scores higher than 50 and represented by more than 3 peptides are listed in Table II.

Discussion

In the present study, using subcellular fractionation of glioma cells, we isolated vesicles related to intracellular transport of HSPG and characterized them with LC-MS. HSPGs and HSPG-dependent endocytosis is suggested to play important roles in progression of malignant gliomas, by affecting the receptor localization or activity and thus regulating the oncogenic signaling pathways. From this point of view, mechanistic understanding of endocytic each step as well characterization of molecules involved in the formation of endocytic complexes is critical for identification of novel druggable targets.

The C6 glioma cells express multiple types of HSPGs, representing both syndecan and glypican family members (Figure 1) which are likely to follow different endocytic

Table II. *List of proteins identified from low-density vesicular fractions with high protein scores*

Types of proteins/name	UniProtKB accession ID	Score	Seq. coverage (%)	No. of peptides	Band no.
Cytoskeleton					
Vimentin	P31000	1752.08	62.20	34	10
Tubulin alpha-1B chain	Q6P9V9	1598.77	63.40	27	10
Ttubulin alpha-1A chain	P68370	1591.05	63.40	27	10
Tubulin beta-5 chain	P69897	1584.22	70.50	30	10
Tubulin beta-2B chain	Q3KRE8	1407.65	63.10	30	10
Tubulin beta-2A chain	P85108	1393.84	63.10	30	10
Tubulin beta-4B chain	Q6P9T8	1373.38	58.70	29	10
Tubulin alpha-1C chain	Q6AYZ1	1145.45	55.00	18	10
Actin, cytoplasmic 1	P60711	880.90	41.90	17	11
Tubulin beta-3 chain	Q4QRB4	871.01	32.20	19	10
Actin, aortic smooth muscle	P62738	590.34	31.60	15	11
Calponin-3	P37397	536.23	38.20	9	12
Vinculin	P86972	513.43	6.90	14	8
Macrophage-capping protein	Q6AYC4	499.50	26.10	8	11
Keratin type II cytoskeletal 5	Q6P6Q2	327.39	11.60	7	10
Keratin, type II cytoskeletal 6A	Q4FZU2	375.26	12.90	7	10
Keratin type II cytoskeletal 1	Q6IMF3	210.25	5.60	3	10
Alpha-actinin-4	Q9QXQ0	273.63	17.10	10	7
Nestin	P21263	192.97	5.50	9	3
Peripherin	P21807	166.91	8.50	4	9
Moesin	O35763	121.76	4.20	3	8
WD repeat-containing protein 1	P21807	115.96	5.80	4	9
Vesicular transport					
Annexin A1	P07150	779.84	52.00	12	17
Annexin A2	Q07936	615.82	47.20	12	16
Annexin A6	P48037	468.26	25.10	12	14
EH domain-containing protein 3	Q8R491	433.00	25.60	9	11
EH domain-containing protein 1	Q641Z6	416.74	21.70	9	10
Programmed cell death 6-interacting protein	P11442	322.41	17.50	7	11
Dynamin-1-like protein	O35303	295.96	12.60	8	8
Ras-related protein Rab-7a	P09527	253.00	48.80	14	8
Arfaptin-1	Q9JHU5	161.75	15.00	11	5
Arf-GAP domain and FG repeat-containing protein 1	Q4KLH5	154.99	8.40	9	3
Ras-related protein Rab-14	P61107	148.62	17.70	14	3
Sorting nexin-1	Q99N27	137.75	8.80	8	4
Clathrin heavy chain 1	Q9QZA2	130.89	34.10	4	6
Ras-related protein Rab-1A	Q6NYB7	115.33	20.50	14	4
Ras-related protein Rab-1B	P10536	96.78	18.40	11	3
Ras-related protein Rab-2A	P05712	94.01	17.50	11	3
Rab GDP dissociation inhibitor beta	P50399	88.04	11.50	11	4
General vesicular transport factor p115	P41542	79.4	5.70	6	4
Motor proteins					
Myosin-9	Q62812	2658.84	34.10	4	61
Myosin-10	Q9JLT0	234.59	3.40	4	6
Enzymes					
Pyruvate kinase PKM	P11980	1170.89	47.10	9	28
Alpha-enolase	P04764	1145.45	49.30	10	18
L-lactate dehydrogenase A chain	P04642	723.89	46.10	12	18
Glyceraldehyde-3-phosphate dehydrogenase	P04797	720.98	42.60	12	15
D-3-phosphoglycerate dehydrogenase	O08651	646.44	25.50	10	12
Fructose-bisphosphate aldolase A	P05065	617.48	40.90	11	11
Calpain-2 catalytic	Q07009	436.34	21.10	8	11
Farnesyl pyrophosphate synthase	P05369	340.91	22.10	11	6

Table II. *Continued*

Table II. *Continued*

Types of proteins/name	UniProtKB accession ID	Score	Seq. coverage (%)	No. of peptides	Band no.
Transketolase	P50137	272.66	9.00	9	6
Phosphoglycerate kinase 1	P16617	222.18	15.80	11	5
Creatine kinase B-type	P07335	217.40	14.40	11	5
Hydroxymethylglutaryl-CoA synthase	P17425	189.33	7.90	10	4
N(G),N(G)-dimethylarginine dimethylaminohydrolase 1	O08557	179.40	24.90	12	7
2',3'-Cyclic-nucleotide 3' phosphodiesterase	P13233	160.40	8.30	11	3
Glucose-6-phosphate isomerase	Q6P6V0	145.54	6.10	10	3
Phospholipase A-2-activating protein	P54319	133.61	6.80	8	4
6-Phosphogluconate dehydrogenase	P85968	127.64	5.20	11	2
Ubiquitinylation-related					
Ubiquitin-like modifier-activating enzyme 1	Q5U300	74.73	5.40	6	4
Nuclear/shuttle proteins					
AH receptor-interacting protein	Q5FWY5	170.46	21.50	12	5
Nucleosome assembly protein 1-like	Q9Z2G8	170.14	4.40	9	3
Importin subunit beta-1	P52296	139.98	9.80	7	6
Nucleophosmin	P13084	116.95	16.80	12	4
Nuclear pore glycoprotein p62	P17955	116.83	7.40	9	3
Importin subunit alpha-5	P83953	105.96	6.90	9	4
Exportin-1	Q80U96	62.73	3.50	6	3
Cell surface receptors					
Neural cell adhesion molecule 1 (NCAM-1)	P13596	84.64	11.20	5	5
Cell signaling					
Ataxin-10	Q9ER24	790.12	38.50	11	17
Serine/threonine-protein kinase PAK 2	Q64303	644.95	30.20	9	14
Dihydropyriminidase-related protein 2	P47942	405.75	19.40	9	8
Mitogen-activated protein kinase 1 (Erk2)	P63086	361.83	26.50	11	9
Serine/threonine-protein kinase PAK 1	P35465	353.42	15.60	9	8
Mitogen-activated protein kinase 3 (Erk1)	Q63844	285.89	23.40	11	7
Glutaredoxin-3	Q9JLZ1	280.91	15.70	11	4
Dual specificity mitogen-activated protein kinase kinase 1	Q01986	267.22	14.50	11	8
Serine/threonine-protein phosphatase 2A regulatory subunit A beta isoform	P36877	204.55	8.80	9	4
cAMP-dependent protein kinase type I-alpha regulatory subunit	Q9JLZ1	185.74	12.30	11	4
Dual specificity mitogen-activated protein kinase kinase 2	P36506	185.30	14.30	11	6
EF-hand domain-containing protein D2	Q4FZY0	131.54	15.90	12	3
Serine/threonine-protein phosphatase 2B catalytic subunit alpha isoform	P63329	119.38	7.30	9	4
Signal transducer and activator of transcription 3 (STAT3)	P52631	87.20	6.40	8	3
Neurochondrin	O35095	70.68	5.50	8	3
Guanine nucleotide-binding protein G(I)/G(S)/G(T) subunit beta-1	P54311	77.51	7.60	12	3
Chaperones					
Heat shock protein HSP 90-beta	P34058	1171.76	43.60	7	32
Heat shock protein HSP 90-alpha	P82995	941.78	37.00	7	24
Heat shock cognate 71 kDa protein	P63018	633.11	30.00	7	15
T-complex protein subunit 1 beta	Q5XIM9	422.00	18.50	10	7
Protein disulfide-isomerase A6	Q63081	340.91	15.90	11	6
78 kDa Glucose-regulated protein (GRP78)	P06761	313.15	16.80	8	9
Peptidyl-prolyl cis-trans isomerase FKBP4	Q9QVC8	227.12	10.50	10	4
Endoplasmin	Q66HD0	104.53	3.50	7	3
Hsp90 co-chaperone Cdc37	Q63692	102.07	8.70	11	3
Peptidyl-prolyl cis-trans isomerase D	Q6DGG0	84.49	10.50	11	4
Others					
Elongation factor 2	P05197	478.20	25.50	7	17

Table II. *Continued*

Table II. *Continued*

Types of proteins/name	UniProtKB accession ID	Score	Seq. coverage (%)	No. of peptides	Band no.
Elongation factor 1-alpha 1	P62630	432.70	27.50	11	12
Peroxiredoxin-1	Q63716	426.12	55.80	14	10
Eukaryotic initiation factor 4A-II	Q5RKI1	403.95	18.70	11	9
Ribonuclease inhibitor	P29315	359.96	18.40	11	8
Eukaryotic peptide release factor subunit 1	Q5U2Q7	280.91	14.60	10	6
Stress-induced-phosphoprotein 1 (STIP1)	O35814	250.41	10.10	9	5
PDZ and LIM domain protein 4	P36202	235.85	20.00	12	6
Protein SET	Q63945	224.29	13.50	11	3
Pachytene checkpoint Protein 2 homolog	Q5XHZ9	213.12	9.70	11	4
Serine/threonine-protein phosphatase 2A 65 kDa regulatory subunit A beta form	Q4QQT4	204.55	8.80	9	4
40S ribosomal protein SA	P38983	115.26	14.20	11	3
Transgelin-2	Q5XFX0	114.44	23.10	14	5
14-3-3 protein epsilon	P62260	112.57	12.90	13	3
Niban-like protein 1	B4F7E8	107.99	7.20	7	4
Transgelin	P31232	96.00	21.90	14	4

routes as reported previously (9). Payne and colleagues showed that proteoglycans follow clathrin- and caveolin-independent internalization (11) using HeLa and kidney cell lines. In the present study, proteins participating in clathrin-dependent endocytosis, *e.g.* clathrin heavy chain 1, annexin 2, annexin 6 or EHD family members (16-19) were identified, suggesting that in glioma cells at least part of HSPG can be endocytosed *via* clathrin-dependent pathway.

Proteomic analysis also revealed a presence of other proteins that originally were not considered to play a role in endocytic events, however recent reports have implied their involvement in vesicular transport. For example, heat shock proteins Hsc70 and Hsp90, initially identified as molecular chaperones, were detected in our HSPG-positive vesicular fraction with high protein scores and represented by a significant number of peptides (Table II). There have been several reports focusing on Hsc70 and Hsp90 involvement in clathrin-dependent endocytosis and vesicle recycling. For example, Jiang et al. reported the interaction of Hsc70 with clathrin and revealed association of chaperones with vesicular membrane (20), while Liu and colleagues found that recycling of α-synuclein was regulated by Rab11a and Hsp90 complex (21). Interestingly, HSPG was shown to mediate the internalization of α-synuclein in an immortalized neuronal progenitor cell line (22), suggesting that both Hsc70 and Hsp90 may also play a role in vesicular trafficking in glioma cells.

One of the most abundant proteins associated with HSPG-positive vesicular fraction was an IF protein, vimentin (Table II). For many years, function of IFs was correlated mainly with their mechanistic properties, however, recent findings suggest the important roles of IFs in cell signaling, motility or organelle positioning (23). For example, vimentin has been shown to play an important role in positioning of Golgi (24), mitochondria (25) or formation of lamellipodia and thus, cell motility (26). In addition, vimentin IFs have been also suggested to play important roles in membrane trafficking. Direct interaction of vimentin with endo-lysosomal compartment, its effect on positioning of specific endo-lysosomal proteins and direct interaction with Rab7a have been reported (27). Our data suggest that vimentin may be also involved in HSPG trafficking.

Cell surface HSPGs play an important role in the uptake of various extracellular ligands and such characteristics could be utilized for delivery of cancer therapeutics to intracellular targets including small interfering RNA (siRNA)–nanoparticle complexes (28) It has been reported that cellular uptake of siRNA is limited by endocytic recycling (29), thus better understanding of complexes formed during endocytosis and determination of all participating molecules is of importance and would likely enable design of vesicles that can escape from recycling. In the present study we succeeded in proteomic analysis of HSPG-positive vesicular fraction of C6 glioma cells, representing transport vesicles. Further detailed characterization of HSPG-rich vesicular compartments will help us understand the nature of HSPG-ligand interactions and to design the tools for targeted delivery of ligands into the cells. Understanding the nature of endocytic complexes could potentially provide useful information to design effective treatment for glioma.

Acknowledgements

The Authors would like to thank Dr. Tetsuro Watabe (Tokyo Medical and Dental University) and Dr. Masaki Yanagishita (Tokyo Medical and Dental University) for their valuable comments and discussion during preparation of this manuscript. This work was supported by JSPS KAKENHI Grants-in-Aid for Scientific Research 23650319 and 26463087 (to K.A.P-I.), and 25463072 (to M.H.Y.).

References

1 Omuro A and DeAngelis LM: Glioblastoma and other malignant gliomas: a clinical review. JAMA *310*: 1842-1850, 2013.
2 Neill T, Schaefer L and Iozzo RV: Decoding the Matrix: Instructive Roles of Proteoglycan Receptors. Biochemistry *54*: 4583-4598, 2015.
3 Sarrazin S, Lamanna WC and Esko JD: Heparan sulfate proteoglycans. Cold Spring Harb Perspect Biol *3*: a004952, 2011.
4 Christianson HC and Belting M: Heparan sulfate proteoglycan as a cell-surface endocytosis receptor. Matrix Biol *35*: 51-5, 2014.
5 Tkachenko E, Lutgens E, Stan RV and Simons M: Fibroblast growth factor 2 endocytosis in endothelial cells proceed *via* syndecan-4-dependent activation of Rac1 and a Cdc42-dependent macropinocytic pathway. J Cell Sci *117*: 3189-3199, 2004.
6 Su G, Meyer K, Nandini CD, Qiao D, Salamat S and Friedl A: Glypican-1 is frequently overexpressed in human gliomas and enhances FGF-2 signaling in glioma cells. Am J Pathol *168*: 2014-2026, 2006.
7 Xu Y, Yuan J, Zhang Z, Lin L and Xu S: Syndecan-1 expression in human glioma is correlated with advanced tumor progression and poor prognosis. Mol Biol Rep *39*: 8979-8985, 2012.
8 Cecchi F, Pajalunga D, Fowler CA, Uren A, Rabe DC, Peruzzi B, Macdonald NJ, Blackman DK, Stahl SJ, Byrd RA and Bottaro DP: Targeted disruption of heparan sulfate interaction with hepatocyte and vascular endothelial growth factors blocks normal and oncogenic signaling. Cancer Cell *22*: 250-262, 2012.
9 Takeuchi Y, Yanagishita M and Hascall VC: Metabolic pathways of heparan sulfate proteoglycans in a rat parathyroid cell line. J Biol Chem *267*: 14677-14684, 1992.
10 Podyma-Inoue KA, Yokote H, Sakaguchi K, Ikuta M and Yanagishita M: Characterization of heparanase from a rat parathyroid cell line. J Biol Chem *277*: 32459-32465, 2002.
11 Payne CK, Jones SA, Chen C and Zhuang X: Internalization and trafficking of cell surface proteoglycans and proteoglycan-binding ligands. Traffic *8*: 389-401, 2007.
12 Fuki IV, Meyer ME and Williams KJ: Transmembrane and cytoplasmic domains of syndecan mediate a multi-step endocytic pathway involving detergent-insoluble membrane rafts. Biochem J *351*: 607-612, 2000.
13 Podyma-Inoue KA, Hara-Yokoyama M, Shinomura T, Kimura T and Yanagishita M: Syndecans reside in sphingomyelin-enriched low-density fractions of the plasma membrane isolated from a parathyroid cell line. PLoS ONE *7*: e32351, 2012.
14 Laemmli UK: Cleavage of structural proteins during the assembly of the head of bacteriophage T4. Nature *227*: 680-685, 1970.
15 Bhuin T and Roy JK: Rab proteins: the key regulators of intracellular vesicle transport. Exp Cell Res *328*: 1-19, 2014.
16 Lauritzen SP, Boye TL and Nylandsted J: Annexins: linking Ca^{2+} signalling to membrane dynamics. Nat Rev Mol Cell Biol *6*: 449-461, 2005.
17 García-Melero A, Reverter M, Hoque M, Meneses-Salas E, Koese M, Conway JR, Johnsen CH, Alvarez-Guaita A, Morales-Paytuvi F, Elmaghrabi YA, Pol A, Tebar F, Murray RZ, Timpson P, Enrich C, Grewal T and Rentero C: Annexin A6 and Late Endosomal Cholesterol Modulate Integrin Recycling and Cell Migration. J Biol Chem *291*: 1320-1335, 2016.
18 Naslavsky N, Rahajeng J, Sharma M, Jovic´ M and Caplan S: Interactions between EHD Proteins and Rab11-FIP2: A role for EHD3 in early endosomal transport. Mol Biol Cell *17*: 163-177, 2006.
19 Soldati T and Schliwa M: Powering membrane traffic in endocytosis and recycling. Nat Rev Mol Cell Biol *7*: 897-908, 2006.
20 Jiang R, Gao B, Prasad K, Greene LE and Eisenberg E: Hsc70 chaperones clathrin and primes it to interact with vesicle membranes. J Biol Chem *275*: 8439-8447, 2000.
21 Liu J, Zhang J-P, Shi M, Quinn T, Bradner J, Beyer R, Chen S and Zhang J: Rab11a and HSP90 regulate recycling of extracellular α-synuclein. J Neurosci *29*: 1480-1485, 2009.
22 Holmes BB, DeVos SL, Kfoury N, Li M, Jacks R, Yanamandra K, Ouidja MO, Brodsky FM, Marasa J, Bagchi DP, Kotzbauer PT, Miller TM, Papy-Garcia D and Diamond MI: Heparan sulfate proteoglycans mediate internalization and propagation of specific proteopathic seeds. Proc Nat Acad Sci USA *110*: E3138-E3147, 2013.
23 Robert A, Hookway C and Gelfand VI: Intermediate filament dynamics: What we can see now and why it matters. Bioessays *38*: 232-243, 2016.
24 Gao Y and Sztul E: A novel interaction of the Golgi complex with the vimentin intermediate filament cytoskeleton. J Cell Biol *152*: 877-893, 2001.
25 Nekrasova OE, Mendez MG, Chernoivanenko IS, Tyurin-Kuzmin PA, Kuczmarski ER, Gelfand VI, Goldman RD and Minina AA: Vimentin intermediate filaments modulate the motility of mitochondria. Mol Biol Cell *22*: 2282-2289, 2011.
26 Helfand BT, Mendez MG, Murthy S, Shumaker DK, Grin B, Mahammad S, Aebi U, Wedig T, Wu YI, Hahn KM, Inagaki M, Herrmann H and Goldman RD: Vimentin organization modulates the formation of lamellipodia. Mol Biol Cell *22*: 1274-1289, 2011.
27 Styers ML, Salazar G, Love R, Peden AA, Kowalczyk AP and Faundez V: The endo-lysosomal sorting machinery interacts with the intermediate filament cytoskeleton. Mol Biol Cell *15*: 5369-5382, 2004.
28 Au JL-S, Yeung BZ, Wientjes MG, Lu z and Wientjes MG: Delivery of cancer theraupeutics to extracellular and intracellular targets: Determinants, barriers, challenges and opportunities. Adv Drug Deliv Rev *97*: 280-301, 2016.
29 Sahay G, Querbes W, Alabi C, Eltoukhy A, Sarkar S, Zurenko C, Karagiannis E, Love K, Chen D, Zoncu R, Buganim Y, Schroeder A, Langer R and Anderson DG: Efficiency of siRNA delivery by lipid nanoparticles is limited by endocytic recycling. Nat Biotechnol *31*: 653-658, 2013.

Received August 5, 2016
Revised September 9, 2016
Accepted September 21, 2016